Journal of Electron Devices, Vol. 10, 2011, pp. 499-505

© JED [ISSN: 1682 -3427]

Journal of Electron Devices
www.jeldev.org

AN EXPLICIT CROSSTALK AWARE DELAY MODELLING FOR ON-CHIP VLSI RLC INTERCONNECT WITH SKIN EFFECT

Vikas Maheshwari[1], Shilpi Lavania[1], D. Sengupta[2], R. Kar[2], D. Mandal[2], A.K. Bhattacharjee[2]

[1] Department of ECE, Hindustan College of Science and Technology, Mathura, U.P., INDIA

[2] Department of ECE, National Institute of Technology, Durgapur-9, West Bengal, INDIA, rajibkarece@gmail.com

Received 25/07/2011, ***accepted 1/09/2011,*** *online 2/09/2011*

Abstract-

This paper presents a novel analytical closed form expression for the crosstalk noise voltage and delay in the presence of skin effect. With the rapid development of high frequency IC technology, a number of high-speed interconnect effects, such as ringing, signal delay, distortion, reflections, and crosstalk, need to be considered during the IC design. Skin effect is one of the high frequency phenomena that can adversely affect the distribution of current density in interconnect because the problem associated with the skin effect is that it attenuates the high frequency components of a signal more than that of the low frequency components. On-Chip interconnect has become the dominant factor in deep sub-micrometer (DSM) integrated circuits (ICs). With increasing levels of on-chip integration, more functional units are integrated onto a single die, such as a multi-core microprocessor and a system-on-chip. Global interconnect, which acts as a communication media among these functional units, plays an increasingly important role and can significantly limit the performance of advanced systems. Accurate noise and delay modelling for RLC lines is thus critical for timing and signal integrity analysis. Skin effect basically affects the resistance and also the inductance, which in turn affects the system integrity in particular and its response as a whole. The current distribution inside the conductor changes as frequency increases. These changes produced in the conductors are known as skin effect. Till now the skin effect has been neglected for the modelling of the on-chip interconnects. But with the increase in frequency to the GHz range, the skin effect has become prominent in performance parameter modelling. In this paper, firstly a crosstalk noise formula for on chip VLSI interconnect has been proposed without considering the skin effect. The voltage response at the output node is analytically derived and then the skin effect on the line resistance is analysed. In this work, the resistance variation due to the skin effect is considered in two wire transmission line model. An explicit closed form expression has been developed for the estimation of cross-talk noise voltage and delay. The correlation between the skin effect and the noise induced is also discussed. The simulation results justify the efficacy of the proposed crosstalk noise aware delay model in the presence of skin effect.

I. INTRODUCTION

The design techniques in sub-micron technologies results in increase of the coupling in interconnections [1]. Since late 80's, there have been a number of significant researches towards better and accurate modelling and characterization of the resistance, capacitance and the inductance of on-chip VLSI interconnect. In recent years, increase in bandwidth requirements have led to the research into low-loss on-chip interconnects, which theoretically can achieve very high bandwidth [2]. For integrated circuits in the deep submicron (DSM) technology, interconnects play an important role in determining the chip performance and signal integrity. In deep submicron design, interconnect delay is shown to be tens to few hundred times larger than the intrinsic gate delay [3]. In order to reduce interconnect delay, wire-sizing is found to be an effective way. On-chip interconnect analysis begins with an in-depth coverage of delay metrics, including the ubiquitous Elmore delay [4] and its many variations. As integrated circuit feature sizes continue to scale well below 0.18µm, active device counts are reaching hundreds of millions [5]. Wire sizing [6] is found to be effective in reducing interconnect delays. As frequency increases, current density within the conductor varies in such a way that it tends to exclude magnetic flux inside the conductor. This situation results in an increase in resistance of the conductor because maximum current is concentrated near the surface and edges of the conductor, and it also results in the effective inductance of the conductor to decrease as frequency increases. These two effects become especially important while modelling the performance of high-speed data signals. Accurate prediction of propagation delay, crosstalk and pulse distortion in high-speed interconnects is strongly dependent on the per-unit parameters' model accuracy. For example, compared to a RLC model, the RC line model may generate an error of up to 30% of the total system [7]. There are a number of approaches available where the on-chip interconnect is modelled as distributed RLC segments for accurate performance parameters modelling [8-15]. But these models do not consider the high frequency skin effect phenomena.

Despite the technological impact of the skin effect, published models are mostly limited to traditional wire structures such as coaxial cables [16-17]. For on-chip and on-board applications, it is important to estimate the effect for single wires rather than complete transmission lines with a rectangular rather than circular cross-section. Skin effect and the change in inductance are inextricably linked. A SPICE model also links these two effects [18]. The simplest model for

an incremental length of transmission line is the basic series inductance L_1 and a lossless shunt capacitance C, with some resistor R_1 in series with the inductance as shown in Figure 1. R_1 can be either fixed or frequency-dependent to account for skin-effect losses. However, this simple model has no provision to change the signal velocity. In another model, part of the series inductance has a shunt resistance across it and is shown in Figure 2. Note that, at low frequencies, the total inductance is simply the sum of L_1 and L_2, and the loss due to shunt resistor R_2 is negligible because its impedance is much higher than that of L_2. As frequency increases, R_2 becomes dominant and causes more losses as the impedance of L_2 increases.

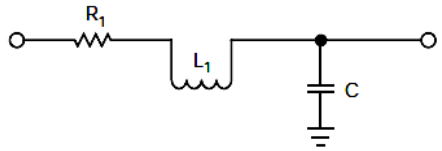

Figure 1. Simple RLC Model

Thus, L_2 and R_2 perform the same function that occurs in a conductor, i.e., as current inside the conductor excludes some of the internal magnetic-flux lines, the apparent inductance decreases, and the loss increases. By changing the values of L_1, L_2, R_1 and R_2, this simple circuit can model the resistance and inductance of an actual conductor.

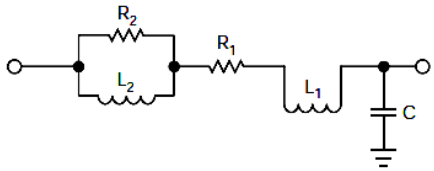

Figure 2. Another type of RLC Model

This paper presents an analytical method for the crosstalk and delay estimation of on-chip VLSI interconnects due to the high frequency of operation where the skin effect has been considered.

The rest of the paper is organized as follows: Basic theory, regarding the previous works and researches are discussed in section 2. Section 3 describes the proposed model for the crosstalk aware delay estimation. Simulation results are shown in Section 4, while Section 5 concludes the paper.

II. BASIC THEORY

The skin effect can be considered at the circuit level as a combination of frequency-dependent resistance and inductance. However, frequency-dependent circuit elements are not suitable for time-domain analysis. Therefore, a circuit representation based on frequency-independent elements is desirable. All circuit models presented in the literatures are based on the ladder topology as shown in Figure-3 or the parallel topology as Figure-4. In both cases, the external inductance L_{ext} is frequency-independent, while the internal impedance (resistance and inductance) is modelled by a combination of resistors and inductors. The external inductance coincides with the asymptotic value of inductance at high frequencies and corresponds to the limit where all current flows on the wire surface and no fields exist inside the wire:

$L_{ext} = L_{hf}$

The internal inductance is the difference between the low- and high-frequency limits [19]:

Lint = $L_{lf} - L_{hf}$; where L_{lf}, L_{hf} are the inductance at low and high frequency, respectively.

This is due to field penetration inside the conductor. Typically, internal inductance accounts for less than 10% of the total low frequency (partial) inductance of a single wire, or open loop [19]. For closely spaced loops, due to cancellation of the self and mutual inductances, the internal inductance can be a significant portion of the loop inductance.

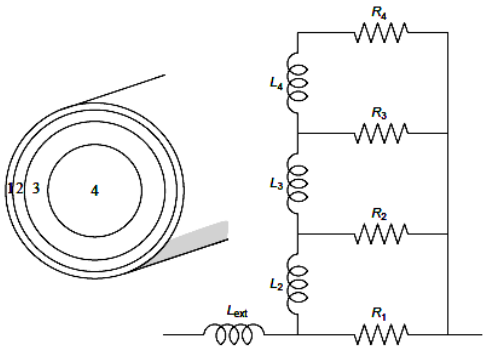

Figure 3. Ladder Topology for Skin Effect

The ladder topology as shown in Figure-3 has been introduced by Wheeler *et al.* [27] and developed by Yen *et al.* [20] and Kim and Neikirk [21]. This topology can be rigorously justified from Maxwell's equations in the quasi-static limit, where each resistor R_i corresponds to a concentric shell in the physical conductor. Exact expressions for the inductances in the case of a circular cross section can be computed for a very fine discretization, i.e., a large number of thin shells [21]. However, no accurate expressions for the L_i's are known for a noncircular cross section, or a small number of shells. Kim and Neikirk [21] developed a technique based on the ad-hoc assumption of a geometric progression of the resistance and inductance values:

$$R_{i+1} = \frac{R_i}{RR}, L_{i+1} = \frac{LL}{L_i} \quad (1)$$

Once R_1 and L_2 are empirically set, the ratios RR and LL are chosen to satisfy constraints on the low frequency resistance R and internal inductance L_{int}. The free parameters in the model are,

$$\alpha_R = \frac{R_1}{R}, \alpha_L = \frac{L_{int}}{L_2} \quad (2)$$

In [21], empirical rules were given to compute α_R and α_L based on wire radius and maximum frequency of operation. These are empirically fitted to exact analytical results or measurements. The fit was performed for a few representative cases; however, no accounting for non-circular geometries was given. Also, estimations of L_{ext} and L_{int} are not discussed except for some special cases.

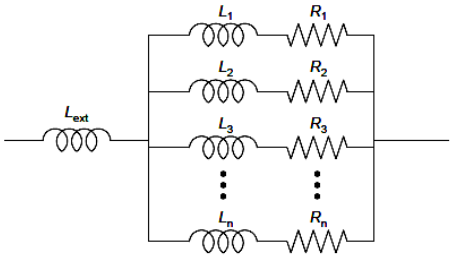

Figure 4. Parallel Topology for Skin-Effect

The parallel *RL* topology, as shown in Figure-4 has no direct physical interpretation. However, due to its simplicity, it is well suited for empirical fit of its parameters to measure data or exact theoretical results. Sen and Wheeler *et al.* [22] proposed a set of rules to determine the parameters R_i and L_i for arbitrary number of parallel branches. Their derivation is similar to that of [21] as both are based on the arbitrary assumption of the geometric scaling of the resistors and inductors and the conservation of R and L_{int}. Also in this case, no estimate was given for L_{ext} and L_{int}. Mei and Ismail [16] used the parallel *RL* topology as a template for the model reduction of a complete, filament-based calculation. However, the model generation requires extensive calculations and no compact expressions are given. In order to assess the efficacy of published models, one needs to find a way to obtain the internal inductance of a wire for a given geometry, without relying on numerical solvers. However, the only formula readily available to estimate internal inductance is valid for a wire with circular cross section and is given in (3).

$$L_{\text{int}} = \frac{\mu l}{8\pi} \tag{3}$$

Choudhury *et al.* [23] considered the internal inductance of a rectangular wire, however, no expressions were provided for a generic aspect ratio. A satisfactory fit [23] for a wire with width W and height H is given in (4).

$$L_{\text{int}} = 10^{-9} l\left[0.3 + 0.28e\left(-0.14\frac{W}{H}\right)\right] \tag{4}$$

where, the wire length l is in centimetres, and $W > H$ (the ratio H/W should be substituted for W/H in the opposite case). It has been verified the accuracy of this expression by comparison with results obtained from Fast Henry [23]. To ensure an accurate numerical modelling, a 20×20 filament matrix has been adopted in the Fast Henry simulations. Note that Fast Henry performs a magneto static calculation, where couplings along the wire length are fully accounted for. The normalized internal inductance is essentially independent of length, but is strongly dependent on the wire aspect ratio. As explained in the next section, this scalability is used to construct a model where all frequency-dependent quantities are independent of length. The figure also compares the analytical fit to (4).

II. PROPOSED WORK

The proposed work is divided in two sub-sections. In the first sub-section, a novel analytical crosstalk model of RLC interconnect is proposed which does not included the skin effect; whereas, in the second sub-section, the skin effect is considered for RLC interconnect modelling. Note that the skin effect makes an adverse effect on the resistance and the inductance. However, this paper only considered the skin effect onto the resistance. The resistance increases with the skin effect; whereas, a decrease in the inductance is accounted.

II. 1 Crosstalk Modelling of RLC Interconnect Analysis Without Skin Effect

In this section a new analytical model of RLC interconnects is proposed. This analysis considers the following interconnect coupling circuit:

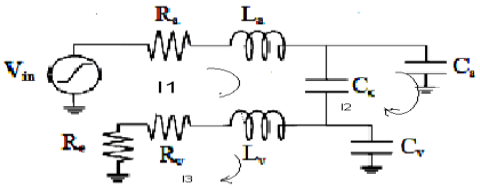

Figure 5. Analytical Model of RLC interconnect

Applying simple loop analysis, the following equations are obtained in terms of RLC:

For first loop:

$$V_{in}(t) = I_1(t).R_a + L_a.\left(\frac{d}{dt}I_1(t)\right) + \frac{1}{C_c}\left[I_1(t) - I_2(t)\right] \tag{5}$$

For second loop:

$$\frac{1}{C_c}[I_2(t) - I_1(t)] - \frac{1}{C_a}I_2(t) = 0 \tag{6}$$

For third loop:

$$R_e I_3(t) + R_v \cdot I_3(t) + L_v \cdot \frac{d}{dt}\left(I_3(t)\right) + \frac{1}{C_c} \cdot I_3(t) = 0 \tag{7}$$

Taking Laplace Transform of (5-7), the following equations are obtained:

$$V_{in}(s) = I_1(s)R_a + sL_aI_1(s) + \frac{[I_1(s) - I_2(s)]}{sC_c} \tag{8}$$

$$\frac{1}{sC_c}[I_2(s) - I_1(s)] - \frac{1}{sC_a}I_2(s) = 0 \tag{9}$$

$$R_eL_3(s) + R_vI_3(s) + sL_vI_3(s) + \frac{1}{sC_v}.I_3(s) = 0 \tag{10}$$

From (9), $$\left[\frac{1}{sC_c} - \frac{1}{sC_a}\right]I_2(s) = \frac{1}{sC_c}I_1(s) \tag{11}$$

Or, $$I_2(s) = \frac{I_1(s)}{sC_c\left(\frac{1}{sC_c} - \frac{1}{sC_a}\right)} \tag{12}$$

So, $I_2(s) = I_1(s)\left(\frac{C_a}{C_a - C_c}\right)$ (13)

From (8),

$$V_{in}(s) = I_1(s).R_a + sL_aI_1(s) + \frac{1}{C_c}I_1(s) - \frac{1}{C_c}I_1(s).\frac{C_a}{C_a - C_c} \quad (14)$$

Or, $V_{in}(s) = I_1(s)\left[R_a + sL_a + \frac{1}{C_c}\left(1 - \frac{C_a}{C_a - C_c}\right)\right]$ (15)

So, $I_1(s) = \frac{V_{in}(s)}{R_a + sL_a + \frac{1}{C_c}\left(1 - \frac{C_a}{C_a - C_c}\right)}$ (16)

With the simple loop analysis it can be found that

$$I_3 = |I_1 - I_2| \quad (17)$$

Therefore, using I_1 and I_2, the third current can be derived which is given as, (18)

$$I_3(s) = \frac{V_{in}(s)C_c}{R_a + sL_a + \frac{1}{C_c}\left(1 - \frac{C_a}{C_a - C_c}\right)(C_a - C_c)}$$

Applying the current divider rule, the current in the victim line capacitor may be found. This finally yields to, (19)

$$I_x = I_3\frac{R_2}{R_1 + R_2}$$

where $R_1 = (R_e + R_v + sL_v) or, R_1 = \frac{1}{sC_v}$

$$I_x = \frac{V_{in}(s)C_c}{R_a + sL_a + \frac{1}{C_c}\left(1 - \frac{C_a}{C_a - C_c}\right)(C_a - C_c)} \times \frac{R_e + R_v + sL_v}{R_e + R_v + sL_v + \frac{1}{sC_v}} \quad (20)$$

The output voltage is given as,

$$V_{co}(s) = I_x \times \frac{1}{sC_v} \quad (21)$$

From (20) and (21) we have,

$$V_{co}(s) = \frac{V_{in}(s)}{sC_v}C_c(R_e + R_v + sL_v)/\left(\left(R_a + sL_a + \frac{1}{C_c\left(1 - \frac{C_a}{C_a - C_c}\right)}\right)\left(R_e + R_v + s\left(L_v + \frac{1}{s.sC_v}\right)\right) \times (C_a - C_c)\right) \quad (22)$$

Some important assumptions that have been made in this paper are as follows:

$$R_e + R_v = A;\ R_a + \frac{1}{C_c}\left[1 - \frac{C_a}{C_a - C_c}\right] = B \quad (23)$$

For step input, $V_{in} = \frac{V_0}{s}$ (24)

Using the above assumptions and applying partial fraction theory yields,

$$V_{co}(s) = \frac{V_0}{s^2(C_a - C_c)}\left[\frac{C_c(A + sL_v)}{(B + sL_a) \times (1 + A + sL_v)}\right] \quad (25)$$

$$S(s) = \frac{F_1}{s} + \frac{F_2}{s^2} + \frac{F_3}{(B + sL_a)} + \frac{F_4}{(1 + A + sL_v)} \quad (26)$$

$$F_1 = \frac{d}{ds}(S(s).s^2)|_{s=0} = \frac{d}{ds}\left[\frac{C_c(A + sL_v)}{(B + sL_a)(1 + A + sL_v)}\right]|_{s=0} \quad (27)$$

$$= \frac{B(A+1)C_cL_v - C_c.A(B.L_v + L_a(A+1))}{\left[B(A+1)^2\right]}$$

$$F_2 = S(s).s^2|_{s=0} = \left(\frac{C_c(A + sL_v)}{(1 + A + sL_v)(B + sL_a)s^2}\right).s^2|_{s=0} = \frac{C_cA}{B(A+1)} \quad (28)$$

$$F_3 = S(s)(B + sL_a)|_{s=-\frac{B}{L_a}} = \frac{C_c(A + sL_v)}{(1 + A + sL_v)s^2}|_{s=-\frac{B}{L_a}} = \frac{C_c\left(A - \frac{B}{L_a}L_v\right)}{\left[(A+1) - \frac{B}{L_a}L_v\right]\left(-\frac{B}{L_a}\right)^2} \quad (29)$$

$$F_4 = S(s)(1 + A + sL_v)|_{s=-\frac{A+1}{L_v}} = \frac{C_c(A + sL_v)}{s^2(B + sL_a)}|_{s=-\frac{(A+1)}{L_v}} \quad (30)$$

$$= -\frac{C_c}{\left[B - (A+1)\frac{L_a}{L_v}\right]\left(\frac{1+A}{L_v}\right)^2}$$

Taking the Laplace inverse transforms of (25) and with the help of (26)-(30), one can derive the explicit expression for $V_{co}(t)$ and it is given in (31).

$$V_{co}(t) = \frac{V}{(C_a - C_c)_0}\left[\left(\frac{B(A+1)C_cL_v - C_cA(BL_v + L_a(A+1))}{[B(1+A)]^2}\right)u(t) + \frac{C_cA}{B(1+A)}.t.u(t) + \frac{C_c\left(A - \frac{B}{L_a}L_v\right)}{\left[(A+1) - \frac{B}{L_a}L_v\right]\left(-\frac{B}{L_a}\right)}e^{-\frac{B}{L_a}t} - \frac{C_c}{\left[B - (1+A)\frac{L_a}{L_v}\right]\left[\frac{A+1}{L_v}\right]^2}e^{-\frac{(1+A)}{L_v}t}\right] \quad (31)$$

The model shown in (31) describes the coupling noise voltage without the presence of skin effect phenomena.

II. 2 Crosstalk Modelling of RLC Interconnect With Skin Effect

In this section, the performance variations of interconnect due to the presence of the skin effect phenomena is considered. The skin effect is the tendency of high frequency current density to be highest at the surface of a conductor and then to decay exponentially towards the centre [24].

The possible reasons for which one must care the skin effect are the following: The resistance of a conductor is inversely proportional to the cross sectional area of the conductor. If the cross sectional area decreases, the resistance goes up. The skin effect causes the effective cross sectional area to decrease. Therefore, the skin effect causes the effective resistance of the conductor to increase [25].

The skin effect is a function of frequency. Therefore, the skin effect causes the resistance of a conductor to become the function of frequency. This, in turn, affects the impedance of the conductor. The inductance decreases as the frequency increases [25]. Let the current is in z-direction and y axis is normal to the interface as shown in the Figure 6.

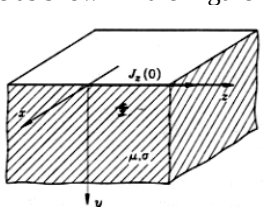

Figure 6. Homogeneous conducting half space

If the angular frequency of the current is ω, and the medium has a conductivity σ, and permeability μ, the complex current density is found to be:

$$J_z(y) = J_z(0).e^{-ky}e^{-jky} \quad (32)$$

where, $k = \sqrt{\frac{\omega\sigma\mu}{2}}$

The intensity of the current density vector decrease exponentially with increasing y. At a distance δ,

$$\delta = \frac{1}{k} = \sqrt{\frac{2}{\omega\mu\sigma}} \quad (33)$$

The amplitude of the current density vector decreases 1/e of its value $J_z(0)$ at the boundary surface. This distance is known as the "skin depth". It is mentioned earlier that only effect of the skin effect on resistance is considered. So for calculating the total effect on the impedance we have to calculate the output impedance. From the Figure 5,

$$Z_1 = \left(\left[R_v + R_e + sL_v\right]\times\frac{1}{sC_v}\right)\Big/\Big/\left((R_v + R_e + sL_v) + \frac{1}{sC_v}\right) \quad (34)$$

$$Z_2 = \frac{(R_v + R_e + sL_v)\times\frac{1}{sC_v}}{(R_v + R_e + sL_v)} + \frac{1}{sC_c} \quad (35)$$

$$Z_3 = \left\{\left(\left[\frac{\left[R_v + R_e + sL_v\right]\times\frac{1}{sC_v}}{\left[R_v + R_e + sL_v + \frac{1}{sC_v}\right]} + \frac{1}{sC_c}\right]\times\frac{1}{sC_a}\right)\Big/\Big/\left(\frac{(R+R+sL)\times\frac{1}{sC}}{(R_v + R_e + sL_v) + \frac{1}{sC_v}} + \frac{1}{sC_c} + \frac{1}{sC_a}\right)\right\} \quad (36)$$

The total output resistance in RLC interconnects is given in (37)

$$Z_0 = \left(\left(\frac{(R+R+sL)\times\frac{1}{sC_v}}{(R_v + R_e + sL_v) + \frac{1}{sC_v}}\right)\times\frac{1}{sC_a}\right)\Big/\Big/\left(\left((R_v + R_e + sL_v)\times\frac{1}{sC_v} + \frac{1}{sC_c} + \frac{1}{sC_a}\right) + (R_a + sL_a)\right) \quad (37)$$

Skin effect on resistance can be calculated by using the following equations:

$$R_{total} = R_{DC} + \sqrt{f}\,R_{AC}, \quad (38)$$

Where, $R_{DC} = \frac{\rho L}{W.t}$ (39)

$$R_{AC} = \frac{\rho L}{A_{current\_densityar\_area}} = \frac{L\rho}{\omega\sqrt{\frac{2}{\omega\sigma\mu}}} = \frac{L\sqrt{\rho}}{\omega\sqrt{2}}\sqrt{\mu f} \quad (40)$$

Therefore, $R = R_{total} = \frac{\rho L}{Wt} + \frac{L\sqrt{\rho}}{\omega\sqrt{2}}.\sqrt{\mu f}$ (41)

It is evident from the above equation that resistance increases as a function of the square root of the frequency due to the skin effect.

Referring to (31), $A_{skin} = A\cdot\sqrt{f}; D = \frac{1}{C_c}\left[1 - \frac{C_a}{C_a - C_c}\right]; B_{skin} = R_a\cdot\sqrt{f} + D$

Thus equation (31) can be used as a source to find the closed form expression of the crosstalk noise with skin effect.

$$V_{co(Skin)}(t) = \frac{V}{(C_a - C_c)_0}\left[\begin{array}{l}\left(\frac{B_{skin}(A_{skin}+1)C_cL_v - C_cA_{skin}(B_{skin}L_v + L_a(A_{skin}+1))}{\left[B_{skin}(1+A_{skin})\right]^2}\right)u(t) + \frac{C_cA_{skin}}{B_{skin}(1+A_{skin})}.t.u(t) + \\ \frac{C_c\left(A_{skin} - \frac{B_{skin}}{L_a}L_v\right)}{\left[(A_{skin}+1) - \frac{B_{skin}}{L_a}L_v\right]\left(-\frac{B_{skin}}{L_a}\right)}e^{-\frac{B_{skin}}{L_a}t} - \frac{C_c}{\left[B_{skin} - (1+A_{skin})\frac{L_a}{L_v}\right]\left[\frac{A_{skin}+1}{L_v}\right]^2}e^{-\frac{(1+A_{skin})}{L_v}t}\end{array}\right] \quad (42)$$

II. 3 Closed Form of Crosstalk Delay Expression in RLC Interconnect With Skin Effect

For the sake of simplification for further analysis, we can consider from (42),

$$p = \left(\frac{B_{skin}(A_{skin}+1)C_cL_v - C_cA_{skin}(B_{skin}L_v + L_a(A_{skin}+1))}{\left[B_{skin}(1+A_{skin})\right]^2}\right); q = \frac{C_cA_{skin}}{B_{skin}(1+A_{skin})};$$

$$r = \frac{C_c\left(A_{skin} - \frac{B_{skin}}{L_a}L_v\right)}{\left[(A_{skin}+1) - \frac{B_{skin}}{L_a}L_v\right]\left(-\frac{B_{skin}}{L_a}\right)}; v = \frac{C_c}{\left[B_{skin} - (1+A_{skin})\frac{L_a}{L_v}\right]\left[\frac{A_{skin}+1}{L_v}\right]^2};$$

$$m = \frac{B_{skin}}{L_a}; n = \frac{(1+A_a)}{L_v}; V_{co(skin)} = \frac{V}{c_a - c_c}\left[p.u(t) + q.u(t) + r.e^{-\frac{B_{skin}}{L_a}.t} - v.e^{-\frac{(1+A_a)}{L_v}.t}\right]$$

For calculation of the delay expression we consider the 50% rise time when $v_2(t)=0.5v_0$. From (21) the general delay expression can be given as,

$$0.5V = \frac{V}{c_a - c_c}\left[p + q + r\left(1 - \frac{B_{skin}}{L_a}.t\right) - v\left(1 - \left(\frac{1+A_a}{L_v}\right).t\right)\right]; 0.5(C_a - C_c) = \left[(p+q+r-v) + t\left(v.\frac{1+A_a}{L_v} - r.\frac{B_{skin}}{L_a}\right)\right]$$

$$t = \frac{\left[0.5(C_a - C_c) - (p+q+r-v)\right]}{v.n - r.m}$$

More simplified form of the delay formula is given as:

$$t = \frac{\left[0.5(C_a - C_c) - (p+q+r-v)\right]}{v.\left(\frac{1+A_a}{L_v}\right) - r.\left(\frac{B_{skin}}{L_a}\right)} \quad (43)$$

The equation (43) shows the proposed model for the crosstalk aware on-chip interconnects delay model.

III. Simulation Results and Discussions

The configuration of circuit for simulation is shown in Figure 5. The high-speed interconnect system consist of two coupled interconnect lines and ground and the length of the lines is d =100 um. These lines are excited by the voltage source of 1.8 V with driver resistance of R_s. The extracted values for the parameters R, L, and C are given in Table 1 [28]. The delays obtained from SPICE are compared with those of the proposed delay model in both the cases i.e. with and without considering the skin effect on the interconnect lines. Tables 2-3 show the comparison of the delay obtained from SPICE with those found using the proposed model without and with considering skin effect, respectively. Note that the difference between the proposed model and the SPICE delay is about 1% in both the cases. Figures 9-10, respectively, show the response of the system with and without considering skin effect, respectively. From these figures we can analyse that the resistance of the interconnect line increases from 120 kΩ to 1560 kΩ due to skin effect.

TABLE I. RLC PARAMETERS FOR A MINIMUM- SIZED WIRES IN A 0.18μM TECHNOLOGY.

Parameter(s)	Value/m
Resistance(R)	120 kΩ/m
Inductance(L)	270 nH/m
Capacitance(C)	240 pF/m
Coupling Capacitance(C_c)	682.49 fF/m

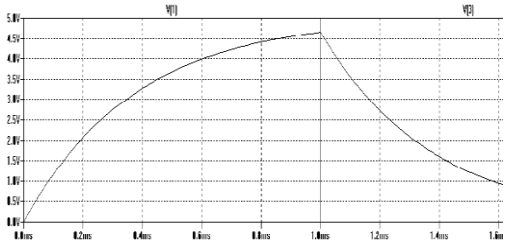

Figure 7. Response of the proposed model with considering Skin Effect R=1560 KΩ

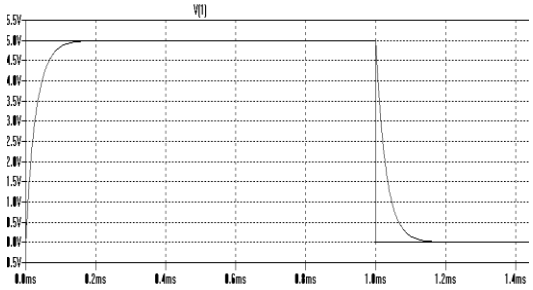

Figure 8. Response of the Proposed model without considering Skin Effect for R=120 KΩ.

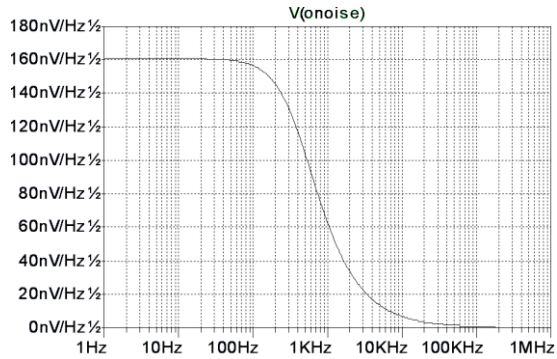

Figure 9. Output node noise with considering skin effect for R=1560 KΩ

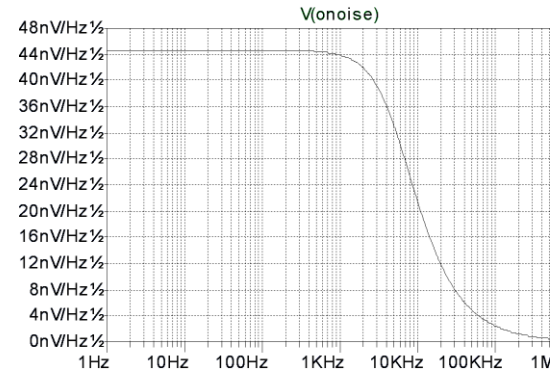

Figure 10. Output node noise without considering skin effect for R=120 KΩ

TABLE II. DELAY WITHOUT SKIN EFFECT

Ex	R_s (KΩ)	C_L (fF)	SPICE Delay (ms)	Proposed Model Delay (ms)
1	1	10	0.1123	0.1141
2	5	50	0.1198	0.1174
3	10	750	0.1479	0.1461
4	50	1000	0.1779	0.1879
5	100	1500	0.1995	0.1998

TABLE III. DELAY WITH SKIN EFFECT

Ex	R_s (KΩ)	C_L (fF)	SPICE Delay (ms)	Proposed Model Delay (ms)
1	1	10	0.1739	0.1867
2	5	50	0.358	0.6567
3	10	750	0.7739	0.8019
4	50	1000	0.8475	0.8912
5	100	1500	0.9757	0.9896

IV. CONCLUSIONS

In this paper, a novel analytical closed form expression for the crosstalk noise modelling with skin effect has been proposed based on the fitting of the transfer function to numerical simulations. We propose a method for the calculation for the skin effect of RLC interconnects. It is shown that skin effect can be computed efficiently in the s-domain using an algebraic formulation, instead of the improper integration in the time domain. The proposed method of computing skin effect relies on the poles and residues of the transfer function and can be used in any kind of model order reduction technique. Compact expressions that describe the skin effect on a single distributed RLC interconnect are rigorously derived. This paper also proposed a novel analytical model for crosstalk and delay to find the impact of the skin effect on the noise in RLC interconnect without considering the skin effect on inductance because the value of the resistance increases dramatically with compared to the value of inductance. Simulation results demonstrate the validity and correctness of our proposed model.

References

[1] L. Gal, "On-Chip Crosstalk-The New Signal Integrity Challenge", IEEE Custom Integrated Circuits Conference, 251-254 (1995).

[2] B. Kleveland, C. Diaz, D. Vook, L. Madden, T. Lee, and S. Wong, "Exploiting CMOS Reverse Interconnect Scaling in Multi-Gigahertz Amplifier and Oscillator Design", IEEE J. Solid-state Circuits, **36**(10), 1480-1488 (2001).

[3] M. Celik, L. Pileggi, A. Odabasioglu, "IC Interconnect Analysis", by Kluwer Academic Publishers (2002).

[4] W. C. Elmore, "The Transient Response of Damped Linear Networks with Particular Regard to Wideband Amplifiers", J. Applied Physics, **19**(1), 55-63 (1948).

[5] S. Y. Wu, B. K. Liew, K.L. Young, C.H. Yu, and S.C. Sun, "Analysis of Interconnect Delay for 0.18µm Technology and Beyond", IEEE International Conference on Interconnect Technology, 68-70 (1999).

[6] M.A. El-Moursy, E.G. Friedman, "Optimum wire sizing of RLC interconnect with repeaters", INTEGRATION, the VLSI journal, **38**, 205–225 (2004).

[7] Y.I. Ismail, E.G. Friedman, "Effects of inductance on the propagation delay and repeater insertion in VLSI circuits", IEEE Trans. on Very Large Scale Integration Systems, **8**(2), 195-206 (2000).

[8] R. Kar, V. Maheshwari, A. Choudhary, A. Singh, "Coupling Aware Explicit Delay Metric for On-Chip RLC Interconnect for Ramp input", International Journal of Signal & Image Processing (IJSIP), **1**(2), 14-19 (2010).

[9] M. Datta, S. Sahoo, D. Ghosh, R. Kar, "An Accurate Analytical Crosstalk Model for On-Chip VLSI RLC Interconnect", International Journal of VLSI Design, International Sciences Press, **2**(1), 83-89 (2011).

[10] S. Sahoo, M. Datta, R. Kar, "Delay and Power Estimation for CMOS Inverter Driving RLC Interconnect Loads", WASET International Journal of Electrical and Electronics Engineering, **5**(3), 165-172 (2011).

[11] S. Sahoo, M. Datta, R. Kar, "Closed Form Solution for Delay and Power for a CMOS Inverter Driving RLC Interconnect under step Input", Journal of Electronic Devices, **10**, 464-470, France (2011).

[12] M. Datta, S. Sahoo, D. Ghosh, R. Kar, "An Accurate Analytical Crosstalk Model for On-Chip VLSI RLC Interconnect", International Conference on Communication and Signal Processing (ICCOS'11), 1133-1137, Coimbatore, India (2011).

[13] S. Sahoo, M. Datta, R. Kar, "An Explicit Delay Model for On-Chip VLSI RLC Interconnect", IEEE International Conference on Devices and Communications (ICDeCom-11), 1-6, India (2011).

[14] S. Sahoo, M. Datta, R. Kar , "An Efficient Dynamic Power Estimation Method for On-Chip VLSI Interconnects", 2nd IEEE International Conference on Emerging Applications of Information Technology (EAIT 2011), India, 379-382 (2011).

[15] S. Sahoo, M. Datta, R. Kar, "An Explicit Delay Analysis of RLC Interconnect using Diffusion Equation Model", International Conference on Computational Vision and Robotics (ICCVR-2010), India, 206-213 (2010).

[16] S. Mei, C. Amin, Y.I. Ismail, "Efficient Model Order Reduction Including Skin Effect", DAC 2003, Anaheim, California, 232-237 (2003).

[17] R.L.Wigington, N.S. Nahman, "Transient Analysis of Coaxial Cables Considering Skin Effect", Proceedings of the IRE, **45**(2), 166-174 (1957).

[18] Reference Data for Radio Engineers, Fifth Edition, Howard W Sams and Co (1968).

[19] B. Mukherjee, L. Wang, A. Pacelli, "A Practical Approach to Modeling Skin Effectin On-Chip Interconnects", GLSVLSI'04, Boston, Massachusetts, USA (2004).

[20] C.-S. Yen, Z. Fazarinc, and R. L. Wheeler, "Time-domain skin-effect model for transient analysis of lossy transmission lines", Proc. IEEE, **70**(7), 750–757 (1982).

[21] S. Kim and D. P. Neikirk, "Compact equivalent circuit model for the skin effect", IEEE Intl. Microwave Symposium Digest, 1815–1818 (1996)

[22] B. Sen and R. L. Wheeler, "Skin effects models for transmission line structures using generic SPICE circuit simulators", IEEE Topical Meeting on Electrical Performance of Electronic Packaging, 128–131 (1998).

[23] J. Choudhury, G. S. Seetharaman, and G. H. Massiha, "Accurate modelling of thin-film inductance for nano-chip", Third IEEE Conference on Nanotechnology, 351–355 (2003).

[24] Skin Effect Douglas Brooks, Ultra-cad Design, Inc. http://www.ultracad.com

[25] Modeling Skin effect in Spice Ultracad Designing, C. Deisch, Tellabs Inc.

[26] S. Mei and Y. I. Ismail, "Modelling skin effect with reduced decoupled RL circuits", in Proc. Intl. Symp. on Circuit and Systems (ISCAS 2003), 588–591 (2003).

[27] H. A. Wheeler, "Formulas for the skin effect", Proc. IRE, **30**, 412–424, (1942).

[28] F Charlet, C.Bermond, S.Putot, G. L. Carval, B. Flechet, "Extraction of (R,L,C,G) interconnect parameters in 2D transmission lines using fast and efficient numerical tools", International Conferece on Simulation of Semiconductor Processes and Devices (SISPAD), 87-89 (2000).